

Self-consistent inclusion of disorder in the BCS-BEC crossover near the critical temperature

M. Iskin

Department of Physics, Koç University, Rumelifeneri Yolu, 34450 Sarıyer, İstanbul, Türkiye

(Dated: March 13, 2026)

We develop a systematic theoretical approach to incorporate the effects of a static white-noise disorder into the BCS-BEC crossover near the critical temperature (T_c) of the superfluid transition. Starting from a functional-integral formulation in momentum-frequency space, we derive an effective thermodynamic potential that fully accounts for Gaussian fluctuations of the order-parameter field and its coupling to the disorder potential. The effective action, expanded to second order in both the disorder potential and the bosonic field, naturally involves third- and fourth-order terms arising from the logarithmic expansion near T_c . By providing a controlled description of pairing fluctuations and disorder effects, this formalism correctly recovers the well-established BCS and BEC limits. This ensures a consistent physical foundation for analyzing the entire BCS-BEC crossover, effectively anchoring the intermediate regime between these two analytically robust endpoints. The approach applies equally to continuum and lattice systems and provides a natural framework for generalizations to multiband models.

I. INTRODUCTION

The study of disordered quantum gases has emerged as a powerful setting for exploring the interplay among interactions, coherence and localization in highly controllable environments [1–13]. Ultracold Fermi gases, in particular, provide an ideal platform for realizing the BCS-BEC crossover under tunable conditions [14–17], where both the interaction strength and the disorder potential can be precisely controlled via Feshbach resonances and optical speckle fields. While the crossover is well characterized in clean systems, the combined effects of disorder and strong pairing correlations remain only partially understood [4, 11, 12]. Theoretically, Fermi gases interpolate between two qualitatively distinct limits: on the BCS side, Anderson’s theorem guarantees the robustness of T_c against weak nonmagnetic disorder, whereas on the BEC side, the transition is governed by phase coherence among tightly-bound fermion pairs, which is highly susceptible to localization and incoherence [18–21]. A unified finite-temperature description valid throughout the BCS-BEC crossover is therefore crucial for interpreting cold-atom experiments and for connecting continuum and lattice models of disordered superfluidity. Previous theoretical studies have either focused on the zero-temperature ($T = 0$) superfluid phase [18, 21] or determined T_c through semiclassical analyses performed within the local-density approximation and the replica trick [19]. Other studies have employed diagrammatic methods at the lowest nontrivial order for the normal phase above T_c , complemented by accurate numerical evaluations of the corresponding diagrammatic contributions [20], or have relied on T -matrix approaches [22]. A fully self-consistent treatment valid across the entire crossover region at finite temperatures is still lacking.

Building on a functional-integral framework in momentum-frequency space, we construct an effective thermodynamic potential that incorporates Gaussian fluctuations of the order parameter together with their

coupling to a static disorder potential. Crucially, our formulation provides a fully quantum and systematically controlled approach that captures the effects of weak disorder throughout the BCS-BEC crossover at leading order in the vicinity of T_c , without resorting to the local-density approximation or the replica trick. By expanding the effective action to second order in both the disorder potential and the bosonic field, and by retaining the necessary third- and fourth-order terms in the logarithmic expansion, our approach yields a controlled finite-temperature description that bridges the BCS and BEC regimes. In contrast to the $T = 0$ approach, where disorder couples to bosonic fluctuations via the second-order term [18, 21], these contributions vanish near T_c , making higher-order terms essential. The formalism reproduces known limiting behaviors for weakly-interacting fermions and bosons, recovers the fermionic and bosonic self-energy diagrams of Ref. [20] for the three-dimensional continuum model, and extends beyond them. Applicable to both continuum and lattice systems, the theory provides a natural route for describing the loss of phase coherence near T_c and for connecting microscopic disorder models in ultracold gases with those relevant to superconductors.

Experimental studies of disordered ultracold Fermi gases in the regime of static disorder across the BCS-BEC crossover remain relatively limited [11, 12]. Nevertheless, measurements of dipole oscillations in static speckle potentials have demonstrated that the damping coefficient depends sensitively on the interaction strength, indicating a nontrivial interplay between disorder and pairing correlations [11]. More recently, experiments have explored the interaction-dependent stability of superfluid coherence under controlled optical speckle disorder, including studies of quenched-disorder dynamics [12]. These works highlight the strong sensitivity of interacting superfluids to disorder and demonstrate the feasibility of probing disorder effects across different interaction regimes. The present theory addresses the complemen-

tary regime of weak static disorder near T_c . In this limit, we predict a qualitative change in the disorder-induced shift of T_c across the BCS-BEC crossover: a slight enhancement of T_c on the BCS side and a suppression on the BEC side. This sign change provides a clear equilibrium benchmark for future experiments capable of measuring T_c shifts under controlled weak disorder.

The paper is organized as follows. In Sec. II, we derive the effective thermodynamic potential near T_c . In Sec. III, we discuss the corresponding self-energy corrections for non-interacting Fermi and Bose gases. In Sec. IV, we analyze the number equation and pair propagator in the BCS and BEC limits. In Sec. V, we examine disorder-induced corrections to T_c across the crossover. Finally, in Sec. VI, we summarize the results and outline future directions, with an Appendix detailing disorder corrections to the number equation in the limiting regimes.

II. EFFECTIVE-ACTION APPROACH NEAR T_c

We assume that the disorder potential varies much more slowly than the thermodynamic processes and it depends only on position. For simplicity, we model it as a static, spin-independent white-noise potential and carry out the thermal average before performing the disorder average [10, 21]. In momentum-frequency space, where $q = (\mathbf{q}, iq_\ell)$ with bosonic Matsubara frequencies $q_\ell = 2\pi\ell/\beta$ for $\ell = 0, \pm 1, \pm 2, \dots$, and $\beta = 1/T$ is the inverse temperature in units of $k_B \rightarrow 1$, the disorder potential satisfies the correlations [18, 21]

$$\langle V_{q=0} \rangle_d = 0, \quad (1)$$

$$\langle V_{q'} V_q \rangle_d = \beta \kappa \delta_{q', -q} \delta_{q_\ell 0}, \quad (2)$$

where $\langle \dots \rangle_d$ denotes the statistical average over random disorder realizations, $\kappa \geq 0$ quantifies the disorder strength, and δ_{ij} is the Kronecker delta.

A. Microscopic model

Having a single-band continuum or a Hubbard model in mind, we consider the microscopic Hamiltonian [21]

$$\begin{aligned} \mathcal{H} = & \sum_{\mathbf{k}\sigma} \xi_{\mathbf{k}\sigma} c_{\mathbf{k}\sigma}^\dagger c_{\mathbf{k}\sigma} + \frac{1}{\sqrt{N}} \sum_{\mathbf{k}\mathbf{k}'\sigma} V_{\mathbf{k}-\mathbf{k}'} c_{\mathbf{k}\sigma}^\dagger c_{\mathbf{k}'\sigma} \\ & - \frac{U}{N} \sum_{\mathbf{k}\mathbf{k}'\mathbf{q}} c_{\mathbf{k}+\mathbf{q}/2, \uparrow}^\dagger c_{-\mathbf{k}+\mathbf{q}/2, \downarrow}^\dagger c_{-\mathbf{k}'+\mathbf{q}/2, \downarrow} c_{\mathbf{k}'+\mathbf{q}/2, \uparrow}, \quad (3) \end{aligned}$$

where $c_{\mathbf{k}\sigma}^\dagger$ ($c_{\mathbf{k}\sigma}$) creates (annihilates) a fermion with momentum \mathbf{k} in units of $\hbar \rightarrow 1$ and spin $\sigma = \{\uparrow, \downarrow\}$. The shifted single-particle dispersion $\xi_{\mathbf{k}\sigma} = \varepsilon_{\mathbf{k}\sigma} - \mu$ is measured relative to the chemical potential μ , and satisfies both time-reversal symmetry $\varepsilon_{\mathbf{k}, \uparrow} = \varepsilon_{-\mathbf{k}, \downarrow} \equiv \varepsilon_{\mathbf{k}}$ and inversion symmetry $\varepsilon_{\mathbf{k}} = \varepsilon_{-\mathbf{k}}$. We do not specify the explicit form of $\xi_{\mathbf{k}} = \varepsilon_{\mathbf{k}} - \mu$, as our formulation applies generally to systems obeying the above symmetries. These

conditions are satisfied, for example, in the continuum model with $\varepsilon_{\mathbf{k}} = |\mathbf{k}|^2/(2m)$, in which case the number of lattice sites N is replaced by the system volume \mathcal{V} . In the lattice model, we instead have

$$\varepsilon_{\mathbf{k}} = -\frac{1}{N} \sum_{ij} t_{ij} e^{i\mathbf{k} \cdot \mathbf{r}_{ij}}, \quad (4)$$

where t_{ij} is the hopping parameter from site j to site i and $\mathbf{r}_{ij} = \mathbf{r}_j - \mathbf{r}_i$ denotes their relative position. In the second term, $V_{\mathbf{q}} = V_q/\sqrt{\beta}$ denotes the Fourier component of the disorder potential. The attractive interaction between spin- \uparrow and spin- \downarrow fermions is taken to be contact-like (zero ranged) in the continuum model and onsite in the Hubbard model with coupling strength $U \geq 0$.

We next calculate the grand partition function \mathcal{Z} for a given microscopic realization of the disorder potential, and subsequently perform the statistical average over all disorder realizations [10, 18, 21].

B. Effective Gaussian action

Using the functional-integral formalism in the momentum-frequency representation [18, 21, 23–26], the grand partition function can be expressed as

$$\mathcal{Z} = \int \mathcal{D}[\phi, \phi^*] e^{-\mathcal{S}[\phi, \phi^*]}, \quad (5)$$

where ϕ_q denotes the Fourier component of the complex bosonic field that captures fluctuations of the superfluid order parameter associated with Cooper pairing. In the vicinity of the critical temperature T_c for the superfluid transition, the action can be written as [21]

$$\mathcal{S}(\phi, \phi^*) = \frac{1}{U} \sum_q |\phi_q|^2 - \text{Tr} \ln(-\beta \mathbf{G}^{-1}), \quad (6)$$

which is a formally exact expression, where the trace Tr is taken over both Nambu and momentum-frequency spaces. Since the saddle-point order parameter vanishes (i.e., $\Delta \rightarrow 0$) near T_c , the inverse Nambu-Gor'kov Green's function can be written as $\mathbf{G}_{kk'}^{-1} = \mathcal{G}_k^{-1} \delta_{kk'} - \boldsymbol{\Sigma}_{kk'}$, where

$$\mathcal{G}_k = \begin{pmatrix} \mathcal{G}_k & 0 \\ 0 & -\mathcal{G}_{-k} \end{pmatrix}, \quad (7)$$

$$\boldsymbol{\Sigma}_{kk'} = \frac{1}{\sqrt{\beta N}} \begin{pmatrix} V_{k-k'} & -\phi_{k-k'} \\ -\phi_{k'-k}^* & -V_{k-k'} \end{pmatrix}. \quad (8)$$

Here, $\mathcal{G}_k = 1/(ik_n - \xi_{\mathbf{k}})$ is the non-interacting Green's function, with $k \equiv (\mathbf{k}, ik_n)$, and fermionic Matsubara frequencies $k_n = (2n+1)\pi/\beta$ for $n = 0, \pm 1, \pm 2, \dots$.

Noting that the non-interacting part is already diagonal in k space, we can first rewrite $\mathbf{G}^{-1} = \mathcal{G}^{-1}(\mathbf{1} - \mathcal{G}\boldsymbol{\Sigma})$, where \mathcal{G} and $\boldsymbol{\Sigma}$ are high-dimensional matrices in k space, and then expand $\ln(\mathbf{1} - \mathcal{G}\boldsymbol{\Sigma}) = -\sum_{n=1}^{\infty} \frac{(\mathcal{G}\boldsymbol{\Sigma})^n}{n}$ to the desired order. In this work, we focus on the effects of weak

disorder on the BCS-BEC crossover formalism. To this end, we must retain terms up to second order in both the disorder potential V_q and the bosonic fields ϕ_q . In contrast to the $T = 0$ case, where it suffices to consider the coupling between disorder and bosonic fluctuations originating from the second-order term in the logarithmic expansion [18, 21], these terms vanish near T_c . Therefore, the third- and fourth-order terms in the expansion must also be included as discussed below.

At the saddle-point level, the zeroth-order action in the logarithmic expansion

$$\mathcal{S}_0 = - \sum_k \text{tr} \ln(-\beta \mathcal{G}_k^{-1}), \quad (9)$$

corresponds to the action of a non-interacting Fermi gas. The first-order action is purely a disorder term proportional to $V_{q=0}$ and therefore averages out from the effective thermodynamic potential. In the second-order action

$$\mathcal{S}_2 = \frac{1}{2} \sum_{k_1 k_2} \text{tr}(\mathcal{G}_{k_1} \Sigma_{k_1 k_2} \mathcal{G}_{k_2} \Sigma_{k_2 k_1}), \quad (10)$$

we separate the usual contribution from the disorder correction and write $\mathcal{S}_2 = \mathcal{S}_2^0 + \mathcal{S}_2^d$. The usual term can be expressed as $\mathcal{S}_2^0 = \sum_{q_1 q_2} A_{q_1 q_2} \phi_{q_1} \phi_{q_2}^*$, where $A_{q_1 q_2} = \Gamma_{q_1}^{-1} \delta_{q_1 q_2}$ is diagonal in q space, and $\Gamma_q^{-1} = \frac{1}{U} - \frac{1}{\beta N} \sum_k \mathcal{G}_{k+q} \mathcal{G}_{-k}$ is the inverse fluctuation propagator in the absence of disorder [23, 27]. It can also be written as

$$\Gamma_q^{-1} = \frac{1}{U} - \frac{1}{N} \sum_{\mathbf{k}} \frac{1 - n_{\text{F}}(\xi_{\mathbf{k}}) - n_{\text{F}}(\xi_{\mathbf{k}+\mathbf{q}})}{iq\ell - \xi_{\mathbf{k}} - \xi_{\mathbf{k}+\mathbf{q}}}, \quad (11)$$

where $n_{\text{F}}(x) = 1/(e^{\beta x} + 1)$ is the Fermi-Dirac distribution function. The saddle-point condition (i.e., the gap equation) near T_c satisfies $\Gamma_0^{-1} = 0$,

$$\frac{1}{U} = \frac{1}{N} \sum_{\mathbf{k}} \frac{1 - 2n_{\text{F}}(\xi_{\mathbf{k}})}{2\xi_{\mathbf{k}}}, \quad (12)$$

and remains unaffected by disorder [18, 19, 21]. Since the disorder correction to the second-order action, $\mathcal{S}_2^d = \frac{1}{2\beta N} \sum_{kq} \text{tr}(\mathcal{G}_k \boldsymbol{\tau}_z \mathcal{G}_{k+q} \boldsymbol{\tau}_z) V_{-q} V_q$, does not couple to ϕ_q , the effective thermodynamic potential depends only on its disorder average, $\langle \mathcal{S}_2^d \rangle_d = \frac{\kappa}{2N} \sum_{kq, q\ell=0} (\mathcal{G}_k \mathcal{G}_{k+q} + \mathcal{G}_{-k} \mathcal{G}_{-k-q})$. Here $\boldsymbol{\tau}_z$ denotes the z component of the Pauli matrices acting in the Nambu-Gor'kov space. In the third-order action

$$\mathcal{S}_3 = \frac{1}{3} \sum_{k_1 k_2 k_3} \text{tr}(\mathcal{G}_{k_1} \Sigma_{k_1 k_2} \mathcal{G}_{k_2} \Sigma_{k_2 k_3} \mathcal{G}_{k_3} \Sigma_{k_3 k_1}), \quad (13)$$

keeping terms up to second order in ϕ_q and V_q , we find $\mathcal{S}_3^d = \sum_{q_1 q_2} B_{q_1 q_2} \phi_{q_1} \phi_{q_2}^*$, where $B_{q_1 q_2} = -\frac{2}{\sqrt{\beta N^3}} \sum_k \mathcal{G}_{k+q_1} \mathcal{G}_{k+q_2} \mathcal{G}_{-k} V_{q_2-q_1}$. Similarly, in

the fourth-order action

$$\mathcal{S}_4 = \frac{1}{4} \sum_{k_1 k_2 k_3 k_4} \text{tr}(\mathcal{G}_{k_1} \Sigma_{k_1 k_2} \mathcal{G}_{k_2} \Sigma_{k_2 k_3} \mathcal{G}_{k_3} \Sigma_{k_3 k_4} \mathcal{G}_{k_4} \Sigma_{k_4 k_1}), \quad (14)$$

keeping terms up to second order in ϕ_q and V_q through straightforward but lengthy algebra, we obtain $\mathcal{S}_4^d = \sum_{q_1 q_2} C_{q_1 q_2} \phi_{q_1} \phi_{q_2}^*$, where $C_{q_1 q_2} = -\frac{1}{\beta^2 N^2} \sum_{k_1 k_2} (2\mathcal{G}_{k_2+q_2} \mathcal{G}_{k_1} \mathcal{G}_{k_2+q_1} \mathcal{G}_{-k_2} + \mathcal{G}_{k_2+q_1} \mathcal{G}_{k_1} \mathcal{G}_{q_2-k_1} \mathcal{G}_{-k_2}) V_{k_2-k_1+q_2} V_{k_1-k_2-q_1}$. As a result, collecting all second-order bosonic terms together, we obtain

$$\mathcal{S}_{\text{B}} = \sum_{q_1 q_2} \Gamma_{\text{B}}^{-1}(q_1, q_2) \phi_{q_1} \phi_{q_2}^*, \quad (15)$$

for the effective Gaussian action, where $\Gamma_{\text{B}}^{-1}(q_1, q_2) = A_{q_1 q_2} + B_{q_1 q_2} + C_{q_1 q_2}$ is the resulting inverse fluctuation propagator in the presence of weak disorder.

C. Effective thermodynamic potential

Next, we obtain the effective thermodynamic potential per lattice site [10, 18, 21]

$$\Omega_{\text{eff}} = -\frac{(\ln \mathcal{Z}_{\text{eff}})_d}{\beta N}, \quad (16)$$

by first integrating out the Gaussian bosonic degrees of freedom and then averaging over the random disorder realizations. To make the discussion more tractable, we separate the fermionic and bosonic contributions and write $\Omega_{\text{eff}} = \Omega_{\text{F}} + \Omega_{\text{B}}$. Furthermore, we separate the usual fermion term from its disorder correction and write $\Omega_{\text{F}} = \Omega_{\text{F}}^0 + \Omega_{\text{F}}^d$. Here, the usual term $\Omega_{\text{F}}^0 = \mathcal{S}_0/(\beta N)$ can be written as

$$\Omega_{\text{F}}^0 = \frac{2}{\beta N} \sum_{\mathbf{k}} \ln[n_{\text{F}}(-\xi_{\mathbf{k}})], \quad (17)$$

which corresponds to the thermodynamic potential of a non-interacting Fermi gas. Similarly, the disorder correction $\Omega_{\text{F}}^d = \langle \mathcal{S}_2^d \rangle_d/(\beta N)$ can be written as

$$\Omega_{\text{F}}^d = \frac{\kappa}{N^2} \sum_{\mathbf{k}\mathbf{q}} \frac{n_{\text{F}}(\xi_{\mathbf{k}}) - n_{\text{F}}(\xi_{\mathbf{k}+\mathbf{q}})}{\xi_{\mathbf{k}} - \xi_{\mathbf{k}+\mathbf{q}}}. \quad (18)$$

Although its form appears quite different, the physical origin of this term is the same as that of the corresponding $T = 0$ result [18, 21]. It corresponds to the Feynman diagram shown in Fig. 1(a).

On the other hand, the bosonic contribution is given by $\Omega_{\text{B}} = \frac{1}{\beta N} \langle \text{Tr} \ln(\Gamma_{\text{B}}^{-1}/\beta) \rangle_d$, where we used the matrix identity $\ln \det \mathbf{M} = \text{Tr} \ln \mathbf{M}$, and Γ_{B}^{-1} is a high-dimensional matrix representation in q space. Noting that the usual term $\mathbf{A} \equiv \Gamma^{-1}$ is already diagonal in q

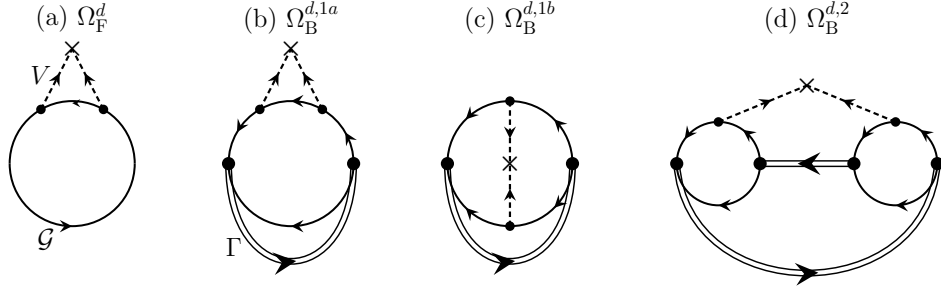


FIG. 1. The diagrammatic representations of the disorder-induced thermodynamic potentials, given by Eqs. (18), (20), (21), and (22), offer an intuitive interpretation of the main theoretical results. In these diagrams, solid, dashed, and double lines represent \mathcal{G}_k , V_q , and Γ_q , respectively.

space, we can first rewrite $\Gamma_B^{-1} = \Gamma^{-1}[\mathbf{1} + \Gamma(\mathbf{B} + \mathbf{C})]$, where \mathbf{B} and \mathbf{C} are again matrix representations in q space, and then separate $\Omega_B = \Omega_B^0 + \Omega_B^d$. Here, the zeroth-order term in the logarithmic expansion,

$$\Omega_B^0 = -\frac{1}{\beta N} \sum_q \ln(\beta \Gamma_q), \quad (19)$$

corresponds to the usual bosonic contribution to the effective thermodynamic potential in the absence of disorder [23, 27]. Since our theory is accurate only up to second order in the disorder potential by construction, we expand the disorder correction $\Omega_B^d = \frac{1}{\beta N} \langle \text{Tr} \ln[\mathbf{1} + \Gamma(\mathbf{B} + \mathbf{C})] \rangle_d$ in powers of $\Gamma(\mathbf{B} + \mathbf{C})$ and keep only the relevant terms. While the first-order term in $\Gamma(\mathbf{B} + \mathbf{C})$ contributes as $\Omega_B^{d,1} = \frac{1}{\beta N} \sum_q \langle \Gamma_q C_{qq} \rangle_d$, the second-order term contributes as $\Omega_B^{d,2} = -\frac{1}{2\beta N} \sum_{qk} \langle \Gamma_q B_{q,q+k} \Gamma_{q+k} B_{q+k,q} \rangle_d$. They can be written as

$$\Omega_B^{d,1a} = -\frac{2\kappa}{\beta^2 N^3} \sum_{qk} \Gamma_q \mathcal{G}_k^2 \mathcal{G}_{q-k} \sum_{\mathbf{p}} \mathcal{G}_{\mathbf{p}-\mathbf{q}, k_n}, \quad (20)$$

$$\Omega_B^{d,1b} = -\frac{\kappa}{\beta^2 N^3} \sum_{qk} \Gamma_q \mathcal{G}_{q+k} \mathcal{G}_{-k} \sum_{\mathbf{p}} \mathcal{G}_{\mathbf{q}-\mathbf{p}, -k_n} \mathcal{G}_{\mathbf{p}, q_\ell + k_n}, \quad (21)$$

$$\Omega_B^{d,2} = -\frac{2\kappa}{\beta^3 N^4} \sum_{qk, k_n=0} \Gamma_q \Gamma_{q+k} \left[\sum_p \mathcal{G}_{q+p} \mathcal{G}_{k+q+p} \mathcal{G}_{-p} \right]^2, \quad (22)$$

where $\Omega_B^{d,1} = \Omega_B^{d,1a} + \Omega_B^{d,1b}$. Unlike the analogous disorder correction at $T = 0$ [18, 21], which has a remarkably simple form, these expressions are considerably more involved because they arise from a higher-order logarithmic expansion. They correspond to the Feynman diagrams shown in Figs. 1(b)-1(d), which admit a clear and intuitive diagrammatic interpretation [28]. In Sec. IV, we show that while Ω_B^d provides the leading-order disorder correction in the BCS limit, it is $\Omega_B^{d,2}$ that dominates in the BEC limit.

III. SELF ENERGY: BCS AND BEC LIMITS

For a non-interacting Fermi gas, the effective self-energy contribution that accounts for the effect of weak disorder at the lowest order in κ is given by [20, 29]

$$\Sigma_k^F = \frac{\kappa}{N} \sum_{\mathbf{p}} \frac{1}{ik_n - \xi_{\mathbf{k}+\mathbf{p}}}. \quad (23)$$

In particular, for the continuum model in three dimensions where we also set $N \rightarrow \mathcal{V}$, by first shifting $\mathbf{p} \rightarrow \mathbf{p} - \mathbf{k}$ this expression can be rewritten as $\Sigma_k^F = -m\kappa\Lambda/\pi^2 + m\kappa(ik_n + \mu) \int_0^\Lambda \frac{dp}{ik_n + \mu - \varepsilon_p}$, where Λ is the momentum cutoff. Since the latter integrand is symmetric, we rewrite it as half of an integral from $-\Lambda$ to Λ , take the limit $\Lambda \rightarrow \infty$, and express it as a contour integral, $\frac{1}{2} \oint \frac{dz}{ik_n + \mu - \varepsilon_z} = -i\pi \frac{\sqrt{m} \text{sign}(k_n)}{\sqrt{2(ik_n + \mu)}}$, where the contour is closed in the upper half-plane. When the imaginary part $\text{Im}\sqrt{ik_n + \mu} \leq 0$, i.e., for $k_n \leq 0$, the poles $z_{\mp} = \mp\sqrt{2m(ik_n + \mu)}$ contribute with residues $\pm\sqrt{m/[2(ik_n + \mu)]}$, respectively. This leads to

$$\Sigma_k^F = -\frac{m\kappa\Lambda}{\pi^2} - i \frac{\kappa(2m)^{3/2}}{4\pi} \sqrt{ik_n + \mu} \text{sign}(k_n), \quad (24)$$

which is in perfect agreement with Eq. (3) of Ref. [20]. Noting that $|k_n| \ll \mu \ll \Lambda^2/(2m)$ in the BCS limit, the second term of Σ_k^F is small and can be neglected. The first term is referred to as Σ_k^F in the rest of the paper. See Sec. IV A for further discussion.

Similarly, for a non-interacting Bose gas composed of tightly-bound fermion pairs, the effective self-energy contribution accounting for the lowest-order effect of disorder is given by [20]

$$Z \Sigma_q^M = \frac{\kappa_M}{N} \sum_{\mathbf{p}} \frac{1}{iq_\ell - \xi_{\mathbf{q}+\mathbf{p}}^M}, \quad (25)$$

where Z is the effective residue of the effective molecules, κ_M denotes their effective disorder strength, and $\xi_{\mathbf{q}}^M = \varepsilon_{\mathbf{q}}^M - \mu_M$ is their effective dispersion, as discussed in Sec. IV B. For the continuum model in three dimensions,

we first follow the same steps leading to Eq. (24), and then note that the real and imaginary parts of the square root satisfy $\text{Re}\sqrt{iq_\ell + \mu_M} = -\text{sign}(q_\ell) \text{Im}\sqrt{-iq_\ell - \mu_M}$ and $\text{Im}\sqrt{iq_\ell + \mu_M} = \text{sign}(q_\ell) \text{Re}\sqrt{-iq_\ell - \mu_M}$. This yields

$$Z \Sigma_q^M = -\frac{m_M \kappa_M \Lambda}{\pi^2} + \frac{\kappa_M (2m_M)^{3/2}}{4\pi} \sqrt{-iq_\ell - \mu_M}, \quad (26)$$

which is in perfect agreement with the point-boson result discussed in Ref. [30]. There is, however, a minor discrepancy with Eq. (11) of Ref. [20] due to an oversimplification in their second term. In Secs. IV B and V, we argue that the diverging first term in Eq. (26) is absorbed into the Thouless condition [20, 30], $\bar{\mu}_M = \mu_M + \frac{\kappa_M}{N} \sum_{\mathbf{q}} \frac{1}{\varepsilon_{\mathbf{q}}} \rightarrow 0^+$, implying that the second term governs the disorder-induced correction to T_c in the BEC limit. This stands in sharp contrast to the BCS limit, where the diverging first term in Eq. (24) determines the corresponding correction to T_c , as discussed next.

IV. NUMBER EQUATION

To ensure that our formalism remains applicable throughout the entire BCS-BEC crossover, covering arbitrarily strong interaction strengths U , we must solve Eq. (12) self-consistently together with the corresponding number equation [18, 21, 23–27]. In this work, we define the number of particles per lattice site as the filling fraction $n = \mathcal{N}/N$, and obtain it through the thermodynamic relation

$$n = -\left. \frac{\partial \Omega_{\text{eff}}}{\partial \mu} \right|_{\beta, N}, \quad (27)$$

which ultimately leads to the number equation $n = n_{\text{F}}^0 + n_{\text{F}}^d + n_{\text{B}}^0 + n_{\text{B}}^d$.

A. Number equation in the BCS limit

Since the bosonic fluctuations do not play a significant role in the BCS limit, we expect $n \gg n_{\text{B}}^0 + n_{\text{B}}^d \rightarrow 0$. Furthermore, from Eq. (17), we find

$$n_{\text{F}}^d = \frac{2}{N} \sum_{\mathbf{k}} n_{\text{F}}(\xi_{\mathbf{k}}), \quad (28)$$

which corresponds to the standard number equation for a non-interacting spin-1/2 Fermi gas. Similarly, from Eq. (18), we obtain

$$n_{\text{F}}^d = \frac{\kappa}{N^2} \sum_{\mathbf{k}, \mathbf{q}} \frac{n'_{\text{F}}(\xi_{\mathbf{k}}) - n'_{\text{F}}(\xi_{\mathbf{k}+\mathbf{q}})}{\xi_{\mathbf{k}} - \xi_{\mathbf{k}+\mathbf{q}}}, \quad (29)$$

which represents the lowest-order disorder correction to the number equation for a non-interacting Fermi gas, where $n'_{\text{F}}(x) = \frac{dn_{\text{F}}(x)}{dx} = -\frac{\beta}{4} \text{sech}^2(\beta x/2)$.

In the BCS limit, where $n \rightarrow n_{\text{F}}^0 + n_{\text{F}}^d$, the leading-order effects of weak disorder can be incorporated into the number equation through the self-energy as

$$n = \frac{2}{\beta N} \sum_{\mathbf{k}} \frac{e^{ik_n 0^+}}{ik_n - \xi_{\mathbf{k}} - \Sigma_{\mathbf{k}}^{\text{F}}} \approx 2 \sum_{\mathbf{k}} n_{\text{F}}(\xi_{\mathbf{k}} + \Sigma_{\mathbf{k}}^{\text{F}}), \quad (30)$$

where we approximate $\Sigma_{\mathbf{k}}^{\text{F}}$ with its first term and refer to it as $\Sigma_{\mathbf{k}}^{\text{F}}$ in the BCS limit, as already discussed in Sec. III. To make this connection explicit, we rewrite Eq. (29) as $n_{\text{F}}^d = \frac{2}{N} \sum_{\mathbf{k}} n'_{\text{F}}(\xi_{\mathbf{k}}) S_{\mathbf{k}}$, where $S_{\mathbf{k}} = \frac{\kappa}{2N} \sum_{\mathbf{q}} \left(\frac{1}{\xi_{\mathbf{k}} - \xi_{\mathbf{k}+\mathbf{q}}} + \frac{1}{\xi_{\mathbf{k}} - \xi_{\mathbf{k}-\mathbf{q}}} \right)$. As an illustration, we now evaluate $S_{\mathbf{k}}$ in the BCS limit for the continuum model in three dimensions. Aligning \mathbf{k} along the z axis and averaging over the directions of \mathbf{q} , we find $S_{\mathbf{k}} = -\frac{m}{2\pi^2 k} \int_0^\Lambda q \ln \left| \frac{q+2k}{q-2k} \right| dq$, where $q = |\mathbf{q}|$ and $\Lambda \rightarrow \infty$ is the momentum cutoff. Using the identity $\int_0^a x \ln \left| \frac{x+1}{x-1} \right| dx = a + \frac{a^2-1}{2} \ln \left| \frac{a+1}{a-1} \right|$ for $a > 1$, and taking the limit $\Lambda/(2k) \gg 1$, which is appropriate for the BCS regime where the region $\xi_{\mathbf{k}} = 0$ provides the dominant contribution in \mathbf{k} space, we obtain $S_{\mathbf{k}} = -m\kappa\Lambda/\pi^2$. This corresponds precisely to $\Sigma_{\mathbf{k}}^{\text{F}}$ at the lowest order. See Appendix A for further discussion. In the theory of disordered metals, such a term is usually regarded as an irrelevant constant that can be absorbed into a redefinition of the chemical potential, i.e., $\bar{\mu} = \mu - \Sigma_{\mathbf{k}}^{\text{F}}$. However, within the context of the BCS-BEC crossover, this simplification is no longer valid, since the renormalization of μ is an essential part of the problem and must be treated explicitly [20].

It is important to clarify the scope of this analysis. In Eq. (30), the fermionic self-energy is retained only through its real, momentum-independent contribution, which yields an ultraviolet-divergent shift of the chemical potential. The imaginary part of the self-energy, associated with quasiparticle lifetime effects induced by disorder [20], is neglected within this leading-order near- T_c treatment. While such lifetime effects and the associated vertex corrections in the particle-particle ladder (Cooperon) channel play a central role in microscopic diagrammatic formulations of Anderson's theorem for disordered BCS superconductors, their self-consistent inclusion lies beyond the Gaussian fluctuation framework employed here. Consequently, the present results should be understood as describing the robustness of the number equation and the transition temperature against weak disorder near T_c , rather than as a full treatment of quasiparticle lifetimes or transport properties in the weak-coupling BCS regime.

In contrast to the non-interacting Fermi gas, we next show that $n \rightarrow n_{\text{B}}^0 + n_{\text{B}}^d \neq 2 \sum_{\mathbf{q}} n_{\text{B}}(\xi_{\mathbf{q}}^M + Z \Sigma_{\mathbf{q}}^M)$ for a non-interacting Bose gas composed of tightly-bound fermion pairs. This inequality arises because the frequency-dependent part of the self-energy provides the dominant contribution, as already discussed in Sec. III. Here, $n_{\text{B}}(x) = 1/(e^{\beta x} - 1)$ denotes the Bose-Einstein distribution function, and $\Sigma_{\mathbf{q}}^M$ refers to $\text{Re} \Sigma_{\mathbf{q}}^M$.

B. Pair propagator in the BEC limit

In the absence of disorder, when $\kappa = 0$, the inverse fluctuation propagator in Eq. (11) reduces to $\Gamma_q^{-1} = \frac{1}{U} + \frac{1}{N} \sum_{\mathbf{k}} \frac{1}{iq_\ell - \xi_{\mathbf{k}} - \xi_{\mathbf{k}+\mathbf{q}}}$ in the BEC limit, where $\mu \rightarrow -\varepsilon_b/2$ [23]. Here, $\varepsilon_b \geq 0$ denotes the binding energy of the tightly-bound fermion pairs, determined from

$$\frac{1}{U} = \frac{1}{N} \sum_{\mathbf{k}} \frac{1}{2\varepsilon_{\mathbf{k}} + \varepsilon_b}. \quad (31)$$

By expanding $\varepsilon_{\mathbf{k}+\mathbf{q}}$ up to second order in \mathbf{q} , and using integration by parts $\sum_{\mathbf{k}} \frac{\partial^2 \varepsilon_{\mathbf{k}}}{\partial k_i \partial k_j} \varepsilon_{\mathbf{k}} = -\sum_{\mathbf{k}} \frac{\partial \varepsilon_{\mathbf{k}}}{\partial k_i} \frac{\partial \varepsilon_{\mathbf{k}}}{\partial k_j}$, we obtain the effective pair propagator

$$\Gamma_q = \frac{Z}{iq_\ell - \xi_{\mathbf{q}}^M}, \quad (32)$$

in the BEC limit, where $\xi_{\mathbf{q}}^M = \varepsilon_{\mathbf{q}}^M - \mu_M$ is the effective dispersion for the fermion pairs and $\mu_M = 2\mu + \varepsilon_b$ is their chemical potential. Here, $\varepsilon_{\mathbf{q}}^M = \frac{1}{2} \sum_{ij} q_i q_j (m_M^{-1})_{ij}$ in the $\mathbf{q} \rightarrow \mathbf{0}$ limit, where $(m_M^{-1})_{ij} = \frac{2}{UN} \sum_{\mathbf{k}} \frac{\partial \varepsilon_{\mathbf{k}}}{\partial k_i} \frac{\partial \varepsilon_{\mathbf{k}}}{\partial k_j}$ is the effective inverse mass tensor for the lattice model [31] and $(m_M^{-1})_{ij} = \delta_{ij}/(2m)$ is for the continuum model. At high \mathbf{q} , similar to Eq. (4), we expect $\varepsilon_{\mathbf{q}}^M = \frac{1}{N} \sum_{ij} t_{ij}^M (1 - e^{i\mathbf{q} \cdot \mathbf{r}_{ij}})$ for the lattice model, where $t_{ij}^M = (m_M^{-1})_{ij}/(2a^2)$ is the effective hopping parameter for the pairs from site j to site i , and a is the lattice spacing.

In Eq. (32), the effective residue of the tightly-bound fermion pairs can be determined via $\frac{1}{Z} = \frac{\partial \Gamma_q^{-1}}{\partial (iq_\ell)} \Big|_{q=0}$, leading to $\frac{1}{Z} = -\frac{1}{N} \sum_{\mathbf{k}} \frac{1}{(2\varepsilon_{\mathbf{k}} + \varepsilon_b)^2}$. For the continuum model in three dimensions, one finds $Z = -8\pi \sqrt{\varepsilon_b/m^3}$ with $\varepsilon_b = 1/(ma_s^2)$, where a_s is the s -wave scattering length in vacuum [20, 23], determined by $\frac{1}{U} = -\frac{m}{4\pi a_s} + \frac{1}{N} \sum_{\mathbf{k}} \frac{1}{2\varepsilon_{\mathbf{k}}}$. For the lattice model, we find $Z = -\varepsilon_b^2$ with $\varepsilon_b = U$. Note that by plugging Eq. (31) into the expression $\Gamma_0^{-1} = 0$ in the BEC limit and taking the derivative of the resultant expression with respect to ε_b , we obtain

$$\frac{1}{Z} = \frac{1}{\beta N} \sum_{\mathbf{k}} \mathcal{G}_{\mathbf{k}}^2 \mathcal{G}_{-\mathbf{k}}, \quad (33)$$

which is an alternative expression for the residue, and is particularly useful in the discussion of Sec. IV C.

Given the pair propagator Eq. (32) for the clean BEC limit, the usual number of tightly-bound fermion pairs can be written as $n_M^0 = -\frac{1}{\beta N} \sum_{\mathbf{q}} e^{iq_\ell 0^+} \frac{\Gamma_{\mathbf{q}}}{Z}$, in the absence of a disorder. The disorder induced self-energy expression Eq. (26) can also be written as $Z\Sigma_{\mathbf{q}}^M = \frac{\kappa_M}{N} \sum_{p, p_n=0} \frac{\Gamma_{\mathbf{q}+p}}{Z}$. Thus, the leading-order disorder correction to the number of tightly-bound fermion pairs is expected to be $n_M^d = -\frac{1}{\beta N} \sum_{\mathbf{q}} e^{iq_\ell 0^+} \frac{\Gamma_{\mathbf{q}}^2 \Sigma_{\mathbf{q}}^M}{Z}$. In the presence of weak disorder, if we define $\bar{\Gamma}_{\mathbf{q}}^{-1} = \Gamma_{\mathbf{q}}^{-1} - \Sigma_{\mathbf{q}}^M$, which is equivalent to replacing $\mu_M \rightarrow \mu_M - Z\Sigma_{\mathbf{q}}^M$ in $\Gamma_{\mathbf{q}}^{-1}$, we find $n_M \rightarrow n_M^0 + n_M^d \approx -\frac{1}{\beta N} \sum_{\mathbf{q}} e^{iq_\ell 0^+} \frac{\bar{\Gamma}_{\mathbf{q}}}{Z}$. Note that the

disorder-generalized Thouless condition $\bar{\Gamma}_0^{-1} = 0$ is also equivalent to $\mu_M = Z\Sigma_0^M$. We next show how these expectations are met by our effective thermodynamic potential in the BEC limit.

C. Number equation in the BEC limit

Since the fermionic degrees of freedom play no significant role in the BEC limit, where the Fermi surface vanishes beyond a finite U , as indicated by μ dropping below the band minimum toward $-\varepsilon_b/2$, we expect $n \gg n_F^0 + n_F^d \rightarrow 0$. Furthermore, from Eq. (19), we find

$$n_B^0 = \frac{2}{N} \sum_{\mathbf{q}} n_B(\xi_{\mathbf{q}}^M), \quad (34)$$

which corresponds to twice the standard number equation for a non-interacting spin-0 Bose gas, i.e., $n_B^0 = 2n_F^0$. Similarly, from Eqs. (20) - (22), we obtain the disorder corrections to the number equation in the BEC limit, noting that the dominant contribution originates from the term containing the largest number of $\Gamma_{\mathbf{q}}$ factors. For instance, in evaluating Eq. (22) for $\Omega_B^{d,2}$, we assume that $|\mu| \gg \varepsilon_{\max}$, where ε_{\max} denotes the particle bandwidth, and that $|\mu| \gg |q_\ell|$ over the relevant bosonic energy scales [32]. Under these conditions, we may approximate $\sum_p \mathcal{G}_{q+p} \mathcal{G}_{k+q+p} \mathcal{G}_{-p} \rightarrow \sum_p \mathcal{G}_p^2 \mathcal{G}_{-p}$, and use Eq. (33), which leads to $\Omega_B^{d,2} \rightarrow -\frac{2\kappa}{\beta N^2} \sum_{qk, k_n=0} \frac{\Gamma_{\mathbf{q}} \Gamma_{\mathbf{q}+k}}{Z^2}$. Thus, we identify

$$n_B^{d,2} = -\frac{2\kappa_M}{\beta N^2} \sum_{qk, k_n=0} \frac{\Gamma_{\mathbf{q}}^2 \Gamma_{\mathbf{q}+k}}{Z^3} \quad (35)$$

as the leading-order disorder correction of $\Omega_B^{d,2}$ to the number equation, where $\kappa_M = 4\kappa$ and $\partial(\Gamma_{\mathbf{q}}/Z)/\partial\mu = -2\Gamma_{\mathbf{q}}^2/Z^2$. The factor of 4 in κ_M reflects that the effective disorder potential for a tightly-bound fermion pair is twice that of an unpaired fermion. Note that Eq. (35) is equivalent to the self-energy correction $Z\Sigma_{\mathbf{q}}^{Bd,2} = \frac{\kappa_M}{N} \sum_{k, k_n=0} \frac{\Gamma_{\mathbf{q}+k}}{Z}$, which corresponds precisely to $\Sigma_{4i-4j}^B(q)$ in Ref. [20].

Similarly, in Eq. (20) for $\Omega_B^{d,1a}$, we identify the sum over \mathbf{p} as the BEC-limit form of the fermionic self-energy $\Sigma_{\mathbf{k}}^F$ in the $|\mu| \rightarrow \infty$ limit. To leading order, it can be approximated as $\frac{\kappa}{N} \sum_{\mathbf{p}} \mathcal{G}_{\mathbf{p}-\mathbf{q}, k_n} \rightarrow \frac{\kappa \Lambda^3}{6\pi^2 \mu}$ for the continuum model in three dimensions [20], leading to $\Omega_B^{d,1a} \rightarrow \frac{\kappa \Lambda^3}{3\pi^2 \beta N |\mu|} \sum_{\mathbf{q}} \frac{\Gamma_{\mathbf{q}}}{Z}$. For the lattice model, the same sum can instead be approximated as $\frac{\kappa}{N} \sum_{\mathbf{p}} \mathcal{G}_{\mathbf{p}-\mathbf{q}, k_n} \rightarrow \frac{\kappa}{\mu}$ in the $U \rightarrow \infty$ limit. The continuum result agrees exactly with Eq. (5) of Ref. [20]. Hence, we obtain

$$n_B^{d,1a} = \frac{2\kappa \Lambda^3}{3\pi^2 \beta N |\mu|} \sum_{\mathbf{q}} \frac{\Gamma_{\mathbf{q}}^2}{Z^2}, \quad (36)$$

as the leading-order disorder correction of $\Omega_B^{d,1a}$ to the number equation for the continuum model. This expression is equivalent to the self-energy correction $Z\Sigma_q^{Bd,1a} = -\frac{\kappa\Lambda^3}{3\pi^2|\mu|}$, which corresponds to twice the $\Sigma_{4h}^B(q)$ term in Ref. [20]. The factor of two arises because Ref. [20] includes two such diagrams in their Fig. 4.

Thus, we conclude that while the leading-order self-energy diagrams associated with our bosonic contributions $\Omega_B^{d,2}$ and $\Omega_B^{d,1a}$ are properly included in Ref. [20], the diagram corresponding to the remaining bosonic term $\Omega_B^{d,1b}$ is absent from their analysis. However, as discussed in Ref. [20], one finds that $\Sigma_q^{Bd,1a} \ll \Sigma_q^{Bd,2}$ in the BEC limit, and the same hierarchy holds for the remaining contribution $\Sigma_q^{Bd,1b}$. Therefore, the leading-order effects of weak disorder near T_c can be incorporated into the number equation through the self-energy as

$$n \rightarrow n_B^0 + n_B^d \approx -\frac{2}{\beta N} \sum_q \frac{e^{iq_\ell 0^+}}{iq_\ell - \xi_q^M - Z\Sigma_q^M}, \quad (37)$$

where $\Sigma_q^M \rightarrow \Sigma_q^{Bd,2}$, or equivalently $n_B^d \rightarrow n_B^{d,2} = 2n_B^d$, in the BEC limit. See Appendix A for further discussion. As discussed in Sec. IV B, this corresponds to the expected number equation for a non-interacting Bose gas of tightly-bound fermion pairs, which can be used to reproduce the correct T_c , as shown next.

V. CRITICAL TEMPERATURE T_c

It turns out that the effect of the disorder potential on T_c differs markedly between a weakly-interacting Fermi gas in the BCS limit and a weakly-interacting Bose gas of tightly-bound fermion pairs in the BEC limit [19, 20]. While the self-energy expressions in Eqs. (24) and (26) may appear superficially similar, a key difference emerges: in the fermionic case, the chemical potential μ is large and positive at T_c , effectively shielding the system from disorder. As a result, T_c is primarily determined by the saddle-point condition Eq. (12), and Anderson's theorem protects the transition temperature from weak disorder at the level of the saddle-point and Gaussian fluctuation analysis. In other words, the presence of a large Fermi surface restricts scattering processes, ensuring that weak disorder has only a minimal effect. In contrast, for tightly-bound fermion pairs in the BEC limit, the effective bosonic chemical potential $\bar{\mu}_M \rightarrow 0^+$ at T_c , leaving them fully exposed to disorder. Since T_c is essentially set by the number equation Eq. (37), rather than by Eq. (12) which fixes $\mu \rightarrow -\varepsilon_b/2$, weak disorder directly affects phase coherence through the emergence of an incoherent component in the pair propagator, characterized by the $\sqrt{-iq_\ell}$ dependence of the bosonic self-energy Σ_q^M . This distinction highlights the fundamental role of quantum statistics in determining the robustness of phase coherence against the disorder potential.

As an illustration, for the continuum model in three dimensions in the BCS limit, Eq. (30) indicates that the chemical potential must be shifted as $\mu \rightarrow \mu + \Sigma_{\mathbf{k}}^F$ to preserve the same particle filling n as in the clean system. Because $\Sigma_{\mathbf{k}}^F < 0$, this shift lowers μ relative to the clean case. Within the BCS-BEC crossover, a reduced chemical potential pushes the system toward the unitarity regime, where T_c is higher. Therefore, inserting this lowered μ into Eq. (12) naturally leads to a slightly enhanced T_c compared to the clean system. Indeed, as reported by the numerical calculations of Ref. [20], on the BCS side of unitarity, the presence of disorder produces an increase of T_c by a few percent, indicating that weak disorder can favor fermion pairing in this regime.

On the other hand, in the BEC limit, direct evaluation of Eq. (34) gives $n_B^0 = 2[m_M T_c / (2\pi)]^{3/2} \zeta(3/2)$, where $\zeta(3/2) = 2.612$ is the Riemann-zeta function, and the leading-order disorder correction is given by Eq. (35). The latter can be calculated either by taking the derivative of Eq. (26) with respect to μ_M , or equivalently by performing the momentum sum over \mathbf{q} via direct integration, using $\int_0^\infty \frac{\sqrt{\varepsilon} d\varepsilon}{(iq_\ell - \varepsilon)^2} = \frac{\pi}{2\sqrt{-iq_\ell}}$ for $q_\ell \neq 0$. This yields $n_B^d = \frac{\kappa_M m_M^3}{2\pi^2} T_c$, where we set $\bar{\mu}_M \rightarrow 0$ and employ $\sum_{q_\ell \neq 0} e^{iq_\ell 0^+} = -1$. The latter identity follows from $\frac{1}{\beta} \sum_{q_\ell} e^{iq_\ell 0^+} = \frac{1}{2\pi i} \oint e^{z0^+} n_B(z) dz = 0$, since the integrand vanishes along the circular periphery when the contour encircling the poles is extended to infinity. Note that the $q_\ell = 0$ frequency does not contribute to the disorder correction, and the arising $1/\sqrt{-iq_\ell}$ factor is exactly canceled by the $\sqrt{-iq_\ell}$ dependence of the bosonic self-energy. See Appendix A for further discussion. As a result, we find

$$\left(\frac{T_c}{T_{c,0}}\right)^{3/2} = 1 - \frac{\kappa_M m_M^3 T_c}{4\pi^2 n_{M,0}}, \quad (38)$$

where $T_{c,0} = \frac{2\pi}{m_M} \left[\frac{n_{M,0}}{\zeta(3/2)}\right]^{2/3}$ is the standard expression for the BEC transition temperature of a clean system, with $n_{M,0} = n/2$. To obtain the leading-order disorder correction, T_c on the right-hand side can be replaced by $T_{c,0}$. Thus, in sharp contrast to the slight enhancement of T_c in the BCS limit, disorder leads to a pronounced suppression of T_c in the BEC regime. This result is in excellent agreement with previous analyses of non-interacting point bosons at the lowest order in the disorder potential [30], as well as with those for tightly-bound fermion pairs [19, 20].

In the BCS-BEC crossover problem, one must solve the saddle-point condition in Eq. (12) together with the number equation in Eq. (27) self-consistently in order to determine T_c and μ as functions of U . Even in the clean case, this procedure is already nontrivial in the crossover regime [23]; the inclusion of disorder renders the problem substantially more involved due to the complicated structure of the corrections appearing in Eqs. (20)-(22). In Ref. [20], a comprehensive numerical analysis of the resulting leading-order self-energy diagrams was carried

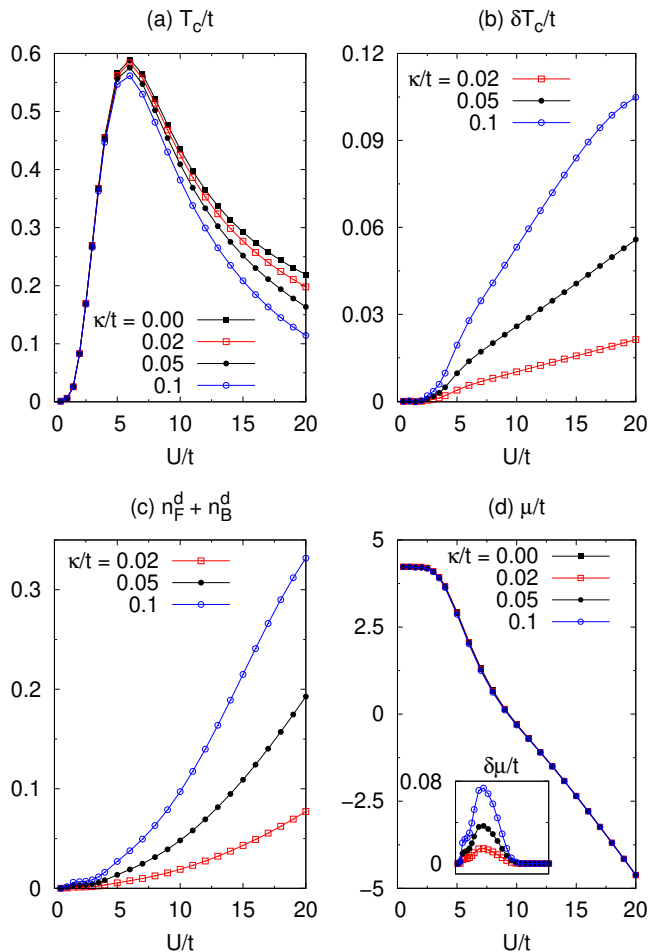


FIG. 2. Self-consistent solutions for (a) the critical temperature T_c , (b) its disorder suppression $\delta T_c = T_{c,0} - T_c$ with $T_{c,0}$ for the clean case, (c) the disorder correction $n_F^d + n_B^d$ to the number equation, and (d) the chemical potential μ . The inset in (d) shows the corresponding disorder correction $\delta\mu = \mu_0 - \mu$, with μ_0 for the clean case. All quantities are plotted as functions of the onsite interaction strength U for $\kappa/t = \{0, 0.02, 0.05, 0.1\}$ at quarter filling ($n = 0.5$).

out across the BCS-BEC crossover under various approximations, together with analytic estimates in the extreme BCS and BEC limits. It was further shown that incorporating disorder effects at the level of Eqs. (30) and (37) provides a qualitatively reliable description in the intermediate regime [19], although quantitative predictions depend sensitively on the specific procedure used to treat cutoff-related issues [20].

As an illustration, in Fig. 2 we consider a cubic lattice with dispersion

$$\varepsilon_{\mathbf{k}} = 2t [3 - \cos(k_x a) - \cos(k_y a) - \cos(k_z a)], \quad (39)$$

where a is the lattice spacing and $t > 0$ is the nearest-neighbor hopping amplitude. We present the self-consistent solutions for T_c , obtained by solving Eq. (12) together with Eqs. (30)

and (37) at quarter filling. Furthermore, we approximate the effective dispersion of fermion pairs as $\varepsilon_{\mathbf{q}}^M = \frac{4t^2}{U} [3 - \cos(q_x a) - \cos(q_y a) - \cos(q_z a)]$, which corresponds to an effective nearest-neighbor hopping $t_M = 2t^2/U$ for the pairs (or, equivalently, an effective mass $m_M = U/(4t^2 a^2)$) and ensures that the interpolation scheme reproduces the correct BEC limit. Thus, while this numerical implementation captures both the BCS and BEC limits by construction, it provides only a qualitative description in the crossover regime. Consistent with our analysis above, the figure shows that the superfluid phase is most robust against disorder in the BCS and crossover regimes, whereas disorder significantly suppresses T_c in the BEC regime. Although this trend is not clearly visible in the figures, we also observe a slight enhancement of T_c in the weak-coupling BCS limit. For example, at $U = 0.5t$, we obtain $T_c \approx 0.000935t$ in the clean case, while $T_c/t \approx \{0.000946, 0.000950, 0.000956\}$ for $\kappa/t = \{0.02, 0.05, 0.1\}$, respectively. However, we note that our numerics do not converge with high precision at such small values of U/t . We further find that the chemical potential μ is reduced relative to its clean-limit value μ_0 in the BCS regime, consistent with the discussion in Sec. IV A. In contrast, in the BEC regime μ is primarily determined by Eq. (12), rather than by Eq. (37), and therefore remains essentially unchanged from its clean-limit value.

Finally, we emphasize that while this Gaussian fluctuation framework provides a systematically controlled description near T_c and recovers the correct BCS and BEC limits, it is not intended for a quantitatively exact treatment of the intermediate crossover. Since Gaussian theories often falter outside their controlled regimes, we employ this approximation to provide a consistent finite-temperature interpolation anchored by analytical limits, rather than a full self-consistent description of spectral properties across the entire crossover.

VI. CONCLUSION

In summary, we developed a systematic theoretical approach that incorporates the effects of weak disorder into the BCS-BEC crossover near the critical temperature T_c . Starting from a functional-integral formulation in momentum-frequency space, we derived an effective thermodynamic potential by expanding the action to second order in both the disorder potential and the bosonic field, which necessitates inclusion of third- and fourth-order terms in the logarithmic expansion near T_c . The resulting formalism fully captures Gaussian fluctuations of the order-parameter field and its coupling to a static white-noise disorder potential. It accurately reproduces the known BCS and BEC limits, recovering the fermionic and bosonic self-energy diagrams identified in Ref. [20] for the three-dimensional continuum model, and extends beyond them. Within this controlled near- T_c framework, the resulting thermodynamic potential and self-energy

expressions provide a consistent leading-order description of the BCS-BEC crossover. By recovering established results for non-interacting point bosons and tightly-bound fermion pairs at the lowest order in disorder [20, 30], this approach enables a systematic interpolation between the weak- and strong-coupling regimes. The predicted crossover from disorder-enhanced to disorder-suppressed T_c provides a clear benchmark for future cold-atom experiments with tunable speckle disorder. Systematic measurements of the transition temperature across the crossover could therefore directly test the self-consistent fluctuation-disorder interplay developed here.

The formalism applies to both continuum and lattice systems and can be naturally extended to multi-band Hubbard models, providing a unified framework for studying the interplay between disorder and interactions. Such generalizations offer a promising route to investigate disorder-induced phenomena in multi-band and quantum-geometric superfluids of strongly-correlated materials [33–35]. The present results capture the leading-order corrections valid in the weak-disorder limit; however, exploring the regime of stronger disorder, where localization effects become significant, remains an important frontier for future investigation.

ACKNOWLEDGMENTS

We thank G. C. Strinati for email correspondence. The author acknowledges funding from US Air Force Office of Scientific Research (AFOSR) Grant No. FA8655-24-1-7391.

Appendix A: Disorder correction to the number equation in the BCS and BEC limits

For the continuum model in three dimensions, it is instructive to comment on the following observation. Since the bosonic self-energy Σ_q^M depends on q_ℓ but not on \mathbf{q} , we may rewrite n_M^d as $\frac{1}{\beta N} \sum_{q_\ell} e^{iq_\ell 0^+} Z \Sigma_q^M \sum_{\mathbf{q}} \frac{\partial}{\partial \mu_M} \left(\frac{1}{iq_\ell - \xi_{\mathbf{q}}^M} \right)$, move the derivative outside the \mathbf{q} sum, and use Eq. (26) for the result of

the \mathbf{q} summation. After setting $\sum_{q_\ell \neq 0} e^{iq_\ell 0^+} = -1$, this procedure yields $\frac{\kappa_M m_M^3}{4\pi^2} T_c$, in full agreement with the result obtained in Sec. V. Note that the $1/\sqrt{-iq_\ell}$ factor is canceled by the $\sqrt{-iq_\ell}$ dependence of Σ_q^M . Therefore, even though the \mathbf{q} sum is formally divergent, the operations $\sum_{\mathbf{q}}$ and $\frac{\partial}{\partial \mu_M}$ happen to commute in this specific calculation.

In the BCS limit, a similar reasoning can be followed. Since the fermionic self-energy Σ_k^F depends on k_n but not on \mathbf{k} , we may rewrite n_F^d as $-\frac{2}{\beta N} \sum_{k_n} e^{ik_n 0^+} \Sigma_k^F \sum_{\mathbf{k}} \frac{\partial}{\partial \mu} \left(\frac{1}{ik_n - \xi_{\mathbf{k}}} \right)$, move the derivative outside the \mathbf{k} sum, and use the alternative expression

$$\Sigma_k^F = -\frac{m\kappa\Lambda}{\pi^2} + \frac{\kappa(2m)^{3/2}}{4\pi} \sqrt{-ik_n - \mu}, \quad (\text{A1})$$

instead of Eq. (24), for the \mathbf{k} summation. After differentiation, this leads to $\frac{(2m)^{3/2}}{4\pi\beta} \sum_{k_n} \frac{e^{ik_n 0^+} \Sigma_k^F}{\sqrt{-ik_n - \mu}}$. Substituting Eq. (A1) produces two distinct terms. The second term vanishes because, when the $\sqrt{-ik_n - \mu}$ factors cancel, the frequency sum can be rewritten as a contour integral over $z = ik_n$, i.e., $\frac{1}{\beta} \sum_{k_n} e^{ik_n 0^+} = -\frac{1}{2\pi i} \oint e^{z 0^+} n_F(z) dz$, which evaluates to zero since the integrand vanishes at the circular periphery when the contour enclosing the poles is extended to infinity. In contrast, for the first term, converting the sum into a contour integral, the integrand exhibits a branch cut for $\text{Re } z > -\mu$, reducing the expression to an integral over the discontinuity $-2i/\sqrt{\varepsilon + \mu}$ across the cut:

$$\sum_{k_n} \frac{e^{ik_n 0^+}}{\sqrt{-ik_n - \mu}} = \frac{-\beta}{2\pi i} \oint \frac{e^{z 0^+} n_F(z) dz}{\sqrt{-z - \mu}} = \frac{\beta}{\pi} \int_{-\mu}^{\infty} \frac{n_F(\varepsilon) d\varepsilon}{\sqrt{\varepsilon + \mu}}. \quad (\text{A2})$$

After integrating by parts, where the boundary terms vanish, the last expression becomes equivalent to the \mathbf{k} sum $-\frac{8\pi\beta}{(2m)^{3/2}N} \sum_{\mathbf{k}} n_F'(\xi_{\mathbf{k}})$. This ultimately leads to $-\frac{2m\kappa\Lambda}{\pi^2\beta N} \sum_{\mathbf{k}} \frac{\partial}{\partial \mu} \sum_{k_n} \frac{e^{ik_n 0^+}}{ik_n - \xi_{\mathbf{k}}}$ for n_F^d , which differs by a minus sign from the correct result. This observation implies that, in this particular case, the operations $\sum_{\mathbf{k}}$ and $\frac{\partial}{\partial \mu}$ anticommute.

-
- [1] S. Ospelkaus, C. Ospelkaus, O. Wille, M. Succo, P. Ernst, K. Sengstock, and K. Bongs, Localization of bosonic atoms by fermionic impurities in a three-dimensional optical lattice, *Physical review letters* **96**, 180403 (2006).
 - [2] G. Modugno, Anderson localization in Bose–Einstein condensates, *Reports on progress in physics* **73**, 102401 (2010).
 - [3] B. Deissler, M. Zaccanti, G. Roati, C. D’Errico, M. Fattori, M. Modugno, G. Modugno, and M. Inguscio, Delocalization of a disordered bosonic system by repulsive interactions, *Nature physics* **6**, 354 (2010).
 - [4] L. Sanchez-Palencia and M. Lewenstein, Disordered quantum gases under control, *Nature Physics* **6**, 87 (2010).
 - [5] S. Kondov, W. McGehee, J. Zirbel, and B. DeMarco, Three-dimensional Anderson localization of ultracold matter, *Science* **334**, 66 (2011).
 - [6] F. Jendrzejewski, A. Bernard, K. Mueller, P. Cheinet, V. Josse, M. Piraud, L. Pezzé, L. Sanchez-Palencia, A. Aspect, and P. Bouyer, Three-dimensional localization of ultracold atoms in an optical disordered potential, *Nature Physics* **8**, 398 (2012).

- [7] S. Krinner, D. Stadler, J. Meineke, J.-P. Brantut, and T. Esslinger, Superfluidity with disorder in a thin film of quantum gas, *Phys. Rev. Lett.* **110**, 100601 (2013).
- [8] S. Krinner, D. Stadler, J. Meineke, J.-P. Brantut, and T. Esslinger, Observation of a fragmented, strongly interacting Fermi gas, *Phys. Rev. Lett.* **115**, 045302 (2015).
- [9] J.-y. Choi, S. Hild, J. Zeiher, P. Schauß, A. Rubio-Abadal, T. Yefsah, V. Khemani, D. A. Huse, I. Bloch, and C. Gross, Exploring the many-body localization transition in two dimensions, *Science* **352**, 1547 (2016).
- [10] A. Cappellaro and L. Salasnich, Superfluids, fluctuations and disorder, *Applied Sciences* **9**, 1498 (2019).
- [11] B. Nagler, K. Jägering, A. Sheikhan, S. Barbosa, J. Koch, S. Eggert, I. Schneider, and A. Widera, Dipole oscillations of fermionic quantum gases along the BEC-BCS crossover in disordered potentials, *Phys. Rev. A* **101**, 053633 (2020).
- [12] J. Koch, S. Barbosa, F. Lang, and A. Widera, Stability and sensitivity of interacting fermionic superfluids to quenched disorder, *Nature Communications* **15**, 9292 (2024).
- [13] P. Russ, M. Yan, N. Kowalski, L. Wadleigh, V. W. Scarola, and B. DeMarco, Compressibility measurement of the thermal MI–BG transition in an optical lattice (2025), [arXiv:2506.16466 \[cond-mat.quant-gas\]](https://arxiv.org/abs/2506.16466).
- [14] S. Giorgini, L. P. Pitaevskii, and S. Stringari, Theory of ultracold atomic Fermi gases, *Rev. Mod. Phys.* **80**, 1215 (2008).
- [15] W. Ketterle and M. W. Zwierlein, Making, probing and understanding ultracold Fermi gases, *La Rivista del Nuovo Cimento* **31**, 247 (2008).
- [16] G. C. Strinati, P. Pieri, G. Röpke, P. Schuck, and M. Urban, The BCS–BEC crossover: From ultra-cold Fermi gases to nuclear systems, *Physics Reports* **738**, 1 (2018).
- [17] T. Hartke, B. Oreg, C. Feng, C. Turnbaugh, J. Hertkorn, Y.-Y. He, N. Jia, E. Khatami, S. Zhang, and M. Zwierlein, Competition of fermion pairing, magnetism, and charge order in the spin-doped attractive Hubbard gas (2025), [arXiv:2511.10605 \[cond-mat.quant-gas\]](https://arxiv.org/abs/2511.10605).
- [18] G. Orso, BCS-BEC crossover in a random external potential, *Phys. Rev. Lett.* **99**, 250402 (2007).
- [19] L. Han and C. A. R. Sá de Melo, Evolution from Bardeen–Cooper–Schrieffer to Bose–Einstein condensate superfluidity in the presence of disorder, *New Journal of Physics* **13**, 055012 (2011).
- [20] F. Palestini and G. C. Strinati, Systematic investigation of the effects of disorder at the lowest order throughout the BCS-BEC crossover, *Phys. Rev. B* **88**, 174504 (2013).
- [21] M. Iskin, Quenched disorder and the BCS-BEC crossover in the Hubbard model, *Phys. Rev. A* **113**, 013312 (2026).
- [22] Y. Che, L. Zhang, J. Wang, and Q. Chen, Impurity effects on BCS-BEC crossover in ultracold atomic Fermi gases, *Phys. Rev. B* **95**, 014504 (2017).
- [23] C. A. R. Sá de Melo, M. Randeria, and J. R. Engelbrecht, Crossover from BCS to Bose superconductivity: Transition temperature and time-dependent Ginzburg-Landau theory, *Phys. Rev. Lett.* **71**, 3202 (1993).
- [24] J. R. Engelbrecht, M. Randeria, and C. A. R. Sá de Melo, BCS to Bose crossover: Broken-symmetry state, *Phys. Rev. B* **55**, 15153 (1997).
- [25] E. Taylor, A. Griffin, N. Fukushima, and Y. Ohashi, Pairing fluctuations and the superfluid density through the BCS-BEC crossover, *Phys. Rev. A* **74**, 063626 (2006).
- [26] R. B. Diener, R. Sensarma, and M. Randeria, Quantum fluctuations in the superfluid state of the BCS-BEC crossover, *Phys. Rev. A* **77**, 023626 (2008).
- [27] P. Nozieres and S. Schmitt-Rink, Bose condensation in an attractive fermion gas: From weak to strong coupling superconductivity, *J. Low Temp. Phys.* **59**, 195 (1985).
- [28] We are grateful to the anonymous referee for pointing out that each of our disorder contributions can be naturally associated with such intuitive Feynman diagrams.
- [29] A. A. Abrikosov, I. Dzyaloshinskii, L. P. Gorkov, and R. A. Silverman, *Methods of quantum field theory in statistical physics* (Dover, New York, NY, 1975).
- [30] A. V. Lopatin and V. M. Vinokur, Thermodynamics of the superfluid dilute Bose gas with disorder, *Phys. Rev. Lett.* **88**, 235503 (2002).
- [31] M. Iskin, Structure factors and quantum geometry in multiband BCS superconductors, *Phys. Rev. B* **112**, 014517 (2025).
- [32] For the three-dimensional continuum model in the BEC limit, the condition $|\mu| \gg \Lambda^2/(2m)$ guarantees that the characteristic pair size ξ_{pair} is much smaller than the disorder correlation length [20]. Since $\xi_{\text{pair}} \propto a_s$ and $|\mu| \simeq 1/(2ma_s^2)$ in this regime, the required separation of length scales is automatically satisfied. An analogous argument applies to the lattice model, where in the strong-coupling limit $U/t \gg 1$ one has $|\mu| \simeq U/2$ and $\varepsilon_{\text{max}} = 12t$, while the pair size scales as $\xi_{\text{pair}} \propto at/U$. Under these conditions, the composite bosons respond to the disorder potential as effectively point-like particles.
- [33] P. Törmä, S. Peotta, and B. A. Bernevig, Superconductivity, superfluidity and quantum geometry in twisted multilayer systems, *Nature Reviews Physics* **4**, 528 (2022).
- [34] J. Yu, B. A. Bernevig, R. Queiroz, E. Rossi, P. Törmä, and B.-J. Yang, Quantum geometry in quantum materials, *npj Quantum Materials* **10**, 101 (2025).
- [35] Y. Jiang, T. Holder, and B. Yan, Revealing quantum geometry in nonlinear quantum materials, *Reports on Progress in Physics* (2025).